Global J. Environ. Sci. Manage. 5(1): 43-60, Winter 2019

Global Journal of Environmental Science and Management
(GJESM)

Homepage: https://www.gjesm.net/

ORIGINAL RESEARCH PAPER

Photodegradation process for the removal of acid orange 10 using titanium dioxide and bismuth vanadate from aqueous solution

B. Rahimi[1], A. Ebrahimi[1,2,*], N. Mansouri[1], N. Hosseini[1]

[1]Department of Environmental Health Engineering, School of Health, Isfahan University of Medical Sciences, Isfahan, Iran

[2]Environment Research Center, Research Institute for Primordial Prevention of Non-communicable disease, Isfahan University of Medical Sciences, Isfahan, Iran

ARTICLE INFO

Article History:
Received 24 June 2018
Revised 22 October 2018
Accepted 17 November 2018

Keywords:
Acid orange 10 (AO10)
Azo dye
Bismuth vanadate ($BiVO_4$)
Photocatalytic degradation
Titanium dioxide (TiO_2)
Visible light

ABSTRACT

In this study, the photocatalytic degradation of azo-dye acid orange 10 was investigated using titanium dioxide catalyst suspension, irradiation with ultraviolet-C lamp and bismuth vanadate under visible light of light-emitting diode lamp. Response surface methodology was successfully employed to optimize the treatment of acid orange 10 dye and assess the interactive terms of four factors. The characteristics of catalysts were determined by field emission scanning electron microscopes, X-ray diffraction and Fourier transform infrared spectroscopy. The optimum values of initial dye concentration, initial pH, irradiation time and catalyst dose were found 11.889 mg/L, 4.592, 12.87 min, and 0.178 g/100 mL for ultraviolet/titanium dioxide process, respectively, and 10.919 mg/L, 3.231, 320.26 min and 0.239 g/100 mL for visible/bismuth vanadate process, respectively. The removal efficiencies obtained for acid orange 10 were 100% and 36.93% after selecting the optimized operational parameters achieved for titanium dioxide and bismuth vanadate, respectively. The highest efficiency was achieved by the use of ultraviolet/titanium dioxide system, while a low acid orange 10 removal efficiency was obtained for the synthesized bismuth vanadate using the co-precipitation method. Thus, it seems necessary to increase the photocatalytic activity of bismuth vanadate in combination with titanium dioxide to remove acid orange 10 dye in subsequent studies.

DOI: 10.22034/gjesm.2019.01.04

INTRODUCTION

By discharging substantial amounts of pollutants into the natural environment, serious soil and water pollution are produced daily (Nong *et al.*, 2011). Several studies have reported that azo dyes are an important category of water soluble artificial colors widely used in textile industry, accounting for 1% to 50% of all commercial dyes (Aleboyeh *et al.*, 2008; Armağan *et al.*, 2003; Saien and Soleymani, 2007). The removal of these pollutants is an important challenge for the environmental engineers. There are aromatic rings in the molecular structures of azo dyes, which make the wastewaters poisonous

*Corresponding Author:
Email: *a_ebrahimi@hlth.mui.ac.ir*
Tel.: +98313 7923280
Fax: +98313 6695849

Note: Discussion period for this manuscript open until April 1, 2019 on GJESM website at the "Show Article.

and largely indestructible as a significant source of environmental pollution (Carmen and Daniela, 2012). A small amount of dyes (below 1 mg/L) has a significant impact on the quality of water (Rafatullah *et al*., 2010). Discharge of such colored effluents into the environment is known as a significant source of pollution causing chemical reactions to occur in the wastewater phase (Udom *et al*., 2013). In general, the effective methods for the treatment of dye-containing sewage can be classified into two types: 1) decoloration by physical and chemical methods, and 2) biodegradation. The traditional physical methods such as activated carbon adsorption, ultrafiltration, reverse osmosis and filtration, which only transfer organic compounds from water into another phase, are applied exceptionally in distillation and extraction (Dawood and Sen, 2012; Ngah *et al*., 2011; Aravind *et al*., 2016). The chemical methods for the removal of dye, such as oxidation-reduction, complexometric methods, ion exchange and neutralization are in fact the processes with a number of advantages and disadvantages (Nickheslat *et al*., 2013; Sohrabi and Ghavami, 2008). Among them, a semiconductor is used as a catalyst in the photocatalytic processes. Crystal structures of TiO_2, including rutile and anatase, have been so far tested in many processes. Only the anatase form of TiO_2 has a high photocatalytic activity, high stability and high value (Fan *et al*., 2012). In UV/TiO_2 system, titanium dioxide absorbs UV light and produces a number of reactive oxygen species (ROS) and hydroxyl radicals ($HO^{\bullet}$) which are very powerful oxidants for degradation of organic pollutants (Zhao *et al*., 2014). The use of TiO_2 is impaired by its wide band gap (3.2 eV) which activates the photocatalysts that respond only to UV light. UV and visible light account for 4% and 45% of solar energy, respectively (Sun *et al*., 2012; Zhen Zhu and Wu, 2015). As compared to the wide band gap counterparts, monoclinic $BiVO_4$ is an ideal photocatalyst which possesses superior performance due to its narrow band gap (2.4 eV) for water oxidation reactions and activates the photocatalysts that only respond to the visible light (Chatchai *et al*., 2009; Natarajan *et al*., 2017). Various studies have been done on the removal of dye by TiO_2 and $BiVO_4$ nanoparticles. Pereira *et al*., (2013) found that the UV/TiO_2 photocatalytic system resulted in the removal of high Xanthene dyes. Using the UV/TiO_2 system. Toor *et al*. (2006) succeeded in removing Direct Yellow 12 dye with 99% removal efficiency in 120 min. Over 40% of 10 mg/L MB dye was degraded by $BiVO_4$ catalyst (0.08g/100 mL) within 360 min in the presence of visible light. (Li *et al*., 2016). Hu *et al*. (2015) also examined the removal of RhB dye by $BiVO_4$ under visible light irradiation. They concluded that the tested catalyst could only remove 34% of the dye from the aqueous solution. The design of experimental (DOE) involves a systematic program for performing surveys conducted by the statistical methods. Using this method, controllable input factors can be systematically changed and their effect on output product parameters can be evaluated. Response surface methodology (RSM) is a set of statistical techniques to build models of experimental and applied mathematics. The purpose of this method is to optimize the output variables which are affected by several input variables (Montgomery, 2009). In the above studies, RSM has been used to optimize the process of dye removal by UV/TiO_2 in a number of cases, including UV/TiO_2 system (Cho and Zoh, 2007; Liu and Chiou, 2005) and UV/TiO_2-coated system (Khataee *et al*., 2011; Vaez *et al*., 2012), but the use of $BiVO_4$ has been very limited. No studies yet have reported on the removal of AO10 dye by RSM using the mentioned nanoparticles. The main objective of this study was to investigate the photocatalytic degradation of an azo dye, called "acid orange 10 (AO10)", in the presence of both TiO_2 particles irradiated by UV-C light and $BiVO_4$ nanoparticles under visible light of LED lamp (light-emitting diode lamp). Therefore, RSM analysis was used to determine various parameters such as initial dye concentration, initial pH, irradiation time, and catalyst dose. Until 1966, AO10 was used as a drug and cosmetic colorant in the USA, but now its application for the mentioned purposes has been stopped because of its potential hazard to humans. Currently, AO10 is used as a colorant in the textile industries (Bonyadinejad *et al*., 2016). This study was performed based on the laboratory data in the Faculty of Health, Isfahan University of Medical Sciences in 2018.

MATERIALS AND METHODS

Materials

AO10 dye was purchased from Sigma Aldrich Company and used without further purification. The molecular formula and molecular weight (g/mol) of AO10 are $C_{16}H_{10}N_2Na_2O_7S_2$ and 452.36, respectively. Fig. 1 displays the structure of this dye. TiO_2 powder (Merck) was used in the experiments

in the anatase form (purity: 99.9 wt%, APS: 20 nm, and SSA: >200 m^2.g). Bismuth nitrate ($Bi(NO_3)_3.5H_2O$) and ammonium metavanadate (NH_4VO_3) were also purchased from Merck(Germany) as precursors of $BiVO_4$. The pH adjustment was done by NaOH and HCl. Distilled water was used to prepare the solution in the whole study.

Synthesis of $BiVO_4$

$BiVO_4$ was prepared using the co-precipitation method. First, 1.17 g NH_4VO_3 and 4.85 g $Bi(NO_3)_3.5H_2O$ were dissolved in 200 mL distilled water. The obtained solution was then mixed at room temperature to reach an orange precipitate. The orange slurry was filtered using filter paper and the residue was washed with distilled water to remove all the ions and salts. The precipitate was dried at 100ºC for 5 h. The final product was calcined at 500ºC for 4 h and then cooled to the room temperature (Fan *et al.*, 2012). Finally, the prepared $BiVO_4$ was kept under a desiccator until application.

Photodegradation procedure

The experimental setup of AO10 dye photo-degradation by TiO_2 and $BiVO_4$ is illustrated in Fig. 2.

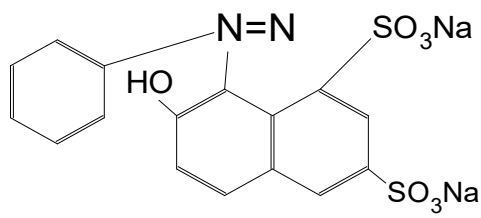

Fig. 1. The studied AO10 chemical structure

TiO_2 experiments

Photocatalytic oxidation of AO10 was carried out in a 100 mL Pyrex glass vessel containing 0.25 g/100 mL catalyst and 10 mg/L AO10 solution. A 125 W high-pressure mercury lamp (Philips) immersed in the inner part of the reactor as a light source. Two mini fans were fixed around the lamps to cool the aqueous solution. Before irradiation, the solution was sonicated for 15 min to disperse TiO_2 uniformity using an ultrasonic (HD 2200 model, Germany Co.). Then, the lamp was turned on to process the required reactions. During irradiation, 4 mL aliquots was withdrawn and then filtered through a 0.22 µm fiberglass filter to remove catalyst particles (Daneshvar *et al.*, 2003; Daneshvar *et al.*, 2004; Pourata *et al.*, 2009).

$BiVO_4$ experiments

Photocatalytic degradation experiments were done by the degradation of AO10 aqueous solution under visible light irradiation and $BiVO_4$ nanoparticles as a photocatalyst. A 12 W LED lamp (white light) located at the top of the reaction vessel was used as a light source. Each experiment was performed at room temperature as follows. 0.25 g of photocatalyst was added into 100 mL of aqueous solution containing 10 mg/L of AO10. Before turning on the LED lamp, it was necessary to sonicate the first mixture for 10 min and later keep it for 1 h in darkness in order to obtain the A010 adsorption/desorption equilibrium by photocatalyst under stirring. At the same irradiation time intervals, a sample (4 mL) was taken from the solution and filtered through a 0.22 µm fiberglass filter to remove the photocatalyst particles (Lili Zhang *et al.*, 2012). The dye decoloration was determined by a spectrophotometer (UV-Vis spectrophotometer,

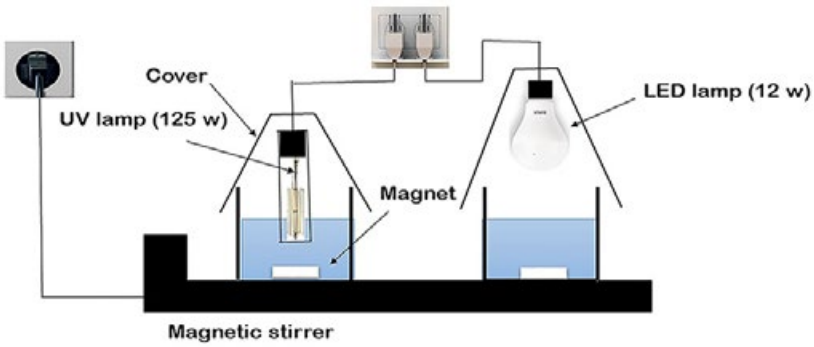

Fig. 2. Experimental setup of AO10 dye photodegradation

DR-5000, HACH LANGE, USA, λ_{max} =475 nm) and a calibration curve (Fig. 3). Eq. 1 was used to calculate the color removal.

$$\text{Color removal}(\%) = \frac{\text{ABS}_0^{475} - \text{ABS}^{475}}{\text{ABS}_0^{475}} \times 100 \quad (1)$$

Where, ABS_0^{475} and ABS^{475} are absorbances at 475 nm before and after treatment, respectively.

Experimental design

Response surface methodology (RSM) is commonly used in the optimization of chemical reactions and/or industrial experimentations to explore nonlinear relationships between continuous predictor variables and the dependent variables. RSM allows for the quadratic surfaces to fit the observed dependent variable values and to determine the predicted maximum (or minimum) values for the dependent variables of interest. In the present study, the rotatable experimental plan was used as a Central Composite Design (CCD) for the optimization of UV/TiO_2 and UV–Vis/$BiVO_4$ treatment of AO10 dye. The effects of four main factors (initial dye concentration, initial pH, irradiation time, and catalyst dosage) on UV/TiO_2 and UV–Vis/$BiVO_4$ processes were investigated. Experimental ranges and levels of

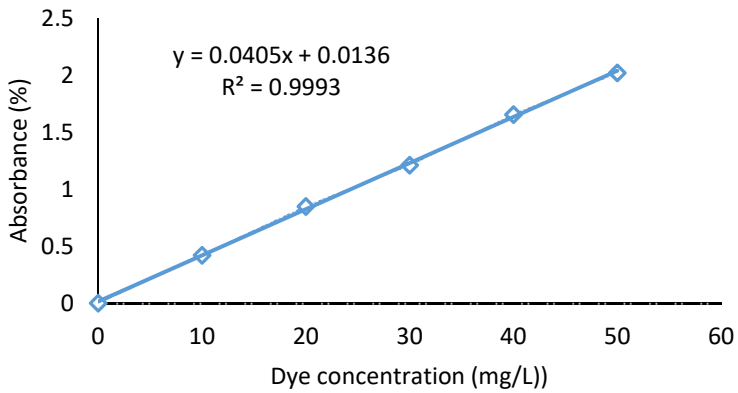

Fig. 3: Calibration curve in wavelength 475 nm

Table 1: Experimental ranges and levels of independent variables for UV/TiO_2 process of AO10 removal

Independent variables	Ranges and levels				
	−2	−1	0	+1	+2
Initial dye concentration (mg/L) (A)	10	20	30	40	50
Initial pH (B)	1	4	7	10	13
Irradiation time (min) (C)	0	5	10	15	20
Catalyst dosage (g/100 mL) (D)	0.05	0.1	0.15	0.2	0.25

Table 2: Experimental range and levels of independent variables for UV–Vis/ $BiVO_4$ process of AO10 removal

Independent variables	Ranges and levels				
	−2	−1	0	+1	+2
Initial dye concentration (mg/L) (A)	10	20	30	40	50
Initial pH (B)	3	4.5	6	7.5	9
Irradiation time (min) (C)	0	90	180	270	360
Catalyst dosage (g/100 mL) (D)	0.05	0.1	0.15	0.2	0.25

independent variables for the studied AO10 removal processes are given in Tables 1 and 2, respectively. For statistical calculations, the value of independent variables X_i (the real value of an independent variable) was coded as x_i (dimensionless coded value of an independent variable) according to Eq. 2.

$$x_i = \frac{X_i - X_0}{\Delta X_i}, \quad i = 1, 2, 3, \ldots, n \qquad (2)$$

Where, x_0 is the value of x_i at the center point, and Δx_i represents the step change.

The data obtained from the experimental runs were analyzed by Design-Expert 10.0.1 software. These data can be presented in graphical forms, or in 3-D response surface and 2-D contour plots. The regression equation related to the quadratic response surface regression design for predicting the optimal conditions is presented by Eq. 3.

$$Y = \beta_0 + \sum_{i=1}^{n} \beta_i x_i + \sum_{i=1}^{n} \beta_{ii} x_i^2 + \sum_{i=1}^{n-1} \sum_{i=j+1}^{n} \beta_{ij} x_i x_j \qquad (3)$$

Where, Y is defined as the response factor for the decolorization efficiency, β_0 is the constant coefficient, β_i, β_{ii}, β_{ij} are the regression coefficients for the linear parameters, quadratic and interaction effect, respectively, and x_i and x_j are the design variables. Furthermore, a successful application of RSM to design optimization of experiment projects can lead to reducing the high cost of analysis methods and their associated numerical noise (Yingling *et al.*, 2011).

RESULTS AND DISCUSSION

Analysis of nanoparticles

The X-ray diffraction (XRD, D8ADVANCE model, Bruker Company, Germany) patterns of nano-TiO_2 in anatase phase and the prepared $BiVO_4$ nanoparticles were obtained by Cu Kα radiation (Figs. 4a and 4b). Field-emission scanning electron microscope (FE-SEM, MIRA3 model, TESCAN Co.) analysis was used to study the shape and uniformity of the nano-TiO_2 and $BiVO_4$ powder samples (Figs. 4c and 4d). It should be noted that the XRD data were collected for both TiO_2 and $BiVO_4$ nanoparticles at diffraction angles of 20° to 80° and 5° to 90°, respectively. There is a strong and sharp diffraction peak at 25.35° in the anatase phase and at 29° for $BiVO_4$ nanoparticles, which can prove that the two nanoparticles conform to the standard samples JCPDS PDF No. 14-0688 and JCPDS PDF No. 21-1272, respectively. TiO_2 nanoparticles are in spherical form and have a size of about 20 nm. However, according to Fig. 4d, the $BiVO_4$ nano-catalyst is completely spherical and uniform and has a size of about 30 nm. FT-IR (Tensor 27-Equinox 55 model, Bruker) has been used to identify functional groups in the catalysts structure in the wavelength range of 400-4000/cm. Based on Fig. 5, TiO_2 and $BiVO_4$ samples have been used for the FT-IR spectrum to study the functional groups. Figs. 5a and 5b shows the spectra related to titanium dioxide and bismuth vanadate in both catalysts with a broad-spectrum in the range of 3400/cm referring to OH groups. Also, in the range of 1630/cm, the presence of bending vibrations of the H_2O molecule adsorbed on the catalyst surface is clearly shown (Venkatachalam *et al.*, 2007). In Fig. 5a, the appearing peak at 600-1000/cm represents the Ti-O vibration (Jian Zhu *et al.*, 2007). In Fig. 5b, the VO_4^{3-} symmetry bending is related to the absorption band at 480/cm. Also, the V-O-V band in the range of 726/cm indicates the stretching vibration (Dong *et al.*, 2014; A Zhang and Zhang, 2009). Fig. 6 confirms the photocatalytic properties of TiO_2 and $BiVO_4$ nanoparticles, which removed the dye from the aqueous solution by UV/ TiO_2 more clearly.

The results of central composite design experiments

The experiments of combined effects of parameters were performed in different conditions using the design of experiments. Experimental plan and results showing the coded values of the variables along with their actual and predicted values are given in Table 3. The regression analyses of AO10 dye removal in terms of coded units are presented in Tables 4 and 5 for UV/ TiO_2 and UV–Vis/$BiVO_4$, respectively. The final equation in terms of coded factors for TiO_2 can be written Eq. 4.

$$Y = +69.22 - 11.69 * A - 1.13 * B + 18.74 * C + 3.32 * D + 0.69 * AB + 0.74 * AC + 0.35 * AD + 0.40 * BC - 0.23 * BD - 0.39 * CD + 1.19 * A^2 + 2.63 * B^2 - 7.36 * C^2 - 0.21 * D^2 \qquad (4)$$

The final equation in terms coded factors for $BiVO_4$ can be expressed by Eq. 5.

$$Y = +25.27292 - 1.07421 * A - 3.30944 * B + 0.065926 * C + 92.59167 * D + 0.069000 * AB - 3.48611 * AC - 2.28250 * AD - 1.38889 * BC + 4.53333 * BD + 0.11694 * CD + 0.012567 * A^2 - 0.017037 * B^2 - 1.13837 * C^2 - 88.33333 * D^2 \qquad (5)$$

Tables 4 and 5 indicate that the coefficients for initial dye concentration (A) (P<0.0001), irradiation time (C) (P<0.0001), and catalyst dose (D) (P=0.0043), except for initial pH (B) (P=0.2691) for TiO_2, are highly significant. However, for $BiVO_4$ all variables are significant. In the quadratic form, B^2 (P=0.0121) and C^2 (P=< 0.0001) for TiO_2 were significant, and A^2 (P<0.0001) and C^2 (P=0.0005) for $BiVO_4$ were highly significant. The interaction terms were not significant for TiO_2 and only AB (P=0.0016), and AD (P=0.0007) were highly significant for $BiVO_4$. ANOVA showed that for TiO_2 and $BiVO_4$, the *P*-values for all models were close to 0, implying that the quadratic models were significant. The values of $R^2_{(adj)}$ for TiO_2 and $BiVO_4$ were 95.26% and 94.91%., respectively, indicating the high accuracy of the model.

Role of TiO_2 in A010 degradation

Fig. 7 shows the effect of UV alone, TiO_2 alone and UV/TiO_2 on contact time in the AO10 dye removal. As can be seen, after 8 min of UV irradiation in the presence of TiO_2, 100% of the dye was degraded. This efficiency decreases to about 84% in the absence of TiO_2 for UV irradiation (photolysis). Fig. 7 also shows

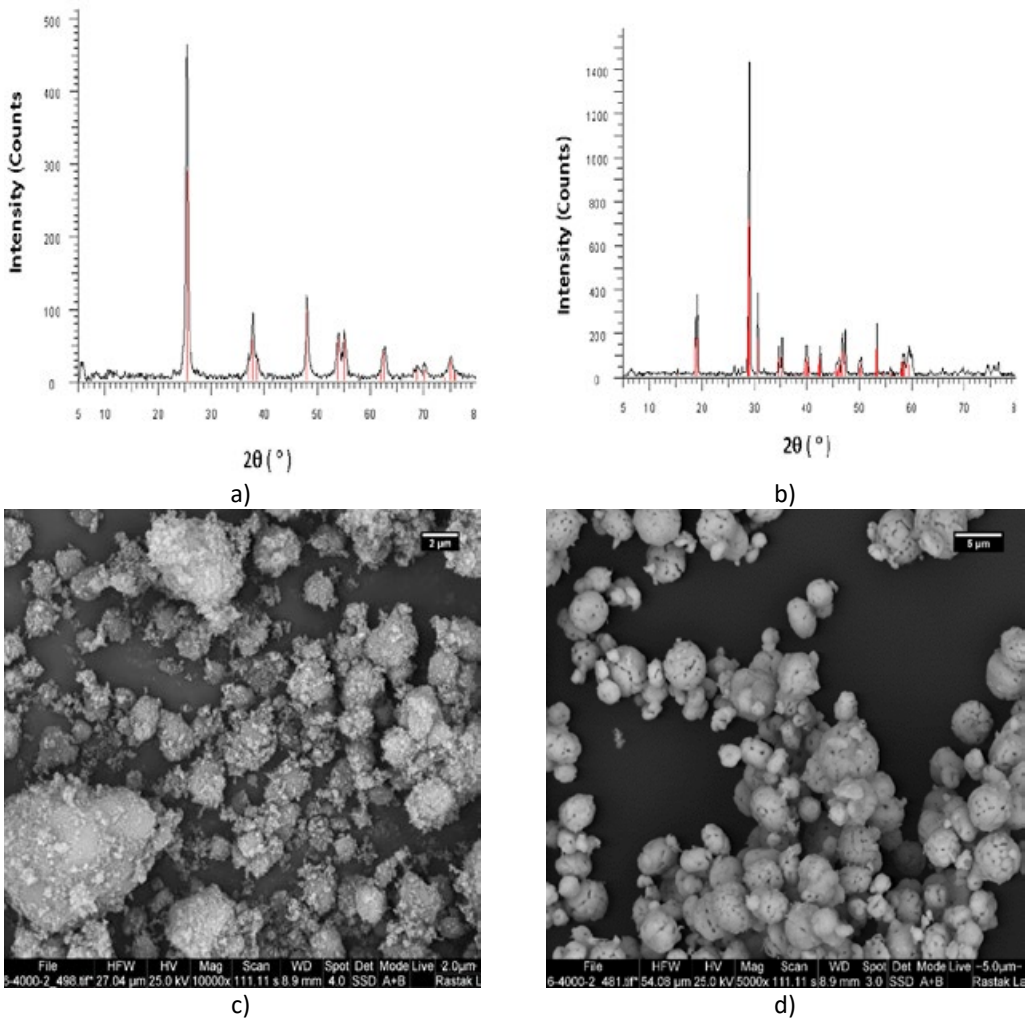

Fig. 4: Characteristics of nano-photocatalysts: a) XRD pattern of nano-TiO_2 in the anatase form; b) XRD pattern of the prepared $BiVO_4$; c) FE-SEM of nano-TiO_2; and d) FE-SEM of the prepared $BiVO_4$

no change in dye concentration when the UV lamp is turned off and TiO_2 particles are used in darkness. In this regards, AO10 was more effectively degraded in the UV/TiO_2 system as compared to the time that either UV or TiO_2 was used alone. The first step in photodegradation by the UV/TiO_2 system is to generate electrons and holes within titanium dioxide particles (Eq. 6). Hydroxyl radicals $(OH)^{\bullet}$ are generated at the surface by valence band (h^+_{VB}), and the conduction band electrons (e^-_{CB}) reduce the amount of oxygen adsorbed onto the surface. Moreover, the generated hydroxyl radicals to attack the organic pollutants are present at or near the surface of TiO_2. They induce the photocatalytic removal of the dye according to Eqs. 7 to 12 (Fujishima *et al.*, 2000; Hoffmann *et al.*, 1995; Jiang and Zhang, 2010;Tang and An, 1995).

$$TiO_2 + hv \rightarrow TiO_2 (e^-_{CB} + h^+_{VB}) \quad (6)$$

$$h^+_{VB} + H_2O_{(ads)} \rightarrow H^+ + OH^*_{(ads)} \quad (7)$$

$$h^+_{VB} + OH^-_{(ads)} \rightarrow OH^*_{(ads)} \quad (8)$$

$$e^-_{CB} + O_{2\,(ads)} \rightarrow {}^{\bullet}O^-_{2\,(ads)} \quad (9)$$

$$OH^*_{(ads)} + \text{dye} \rightarrow \text{degradation of the dye} \quad (10)$$

$$h^+_{VB} + \text{dye} \rightarrow \text{oxidation of dye} \quad (11)$$

$$e^-_{CB} - + \text{dye} \rightarrow \text{reduction of dye} \quad (12)$$

Also, the reactions made by the $BiVO_4$ catalyst in aqueous solution can be similar to those made by

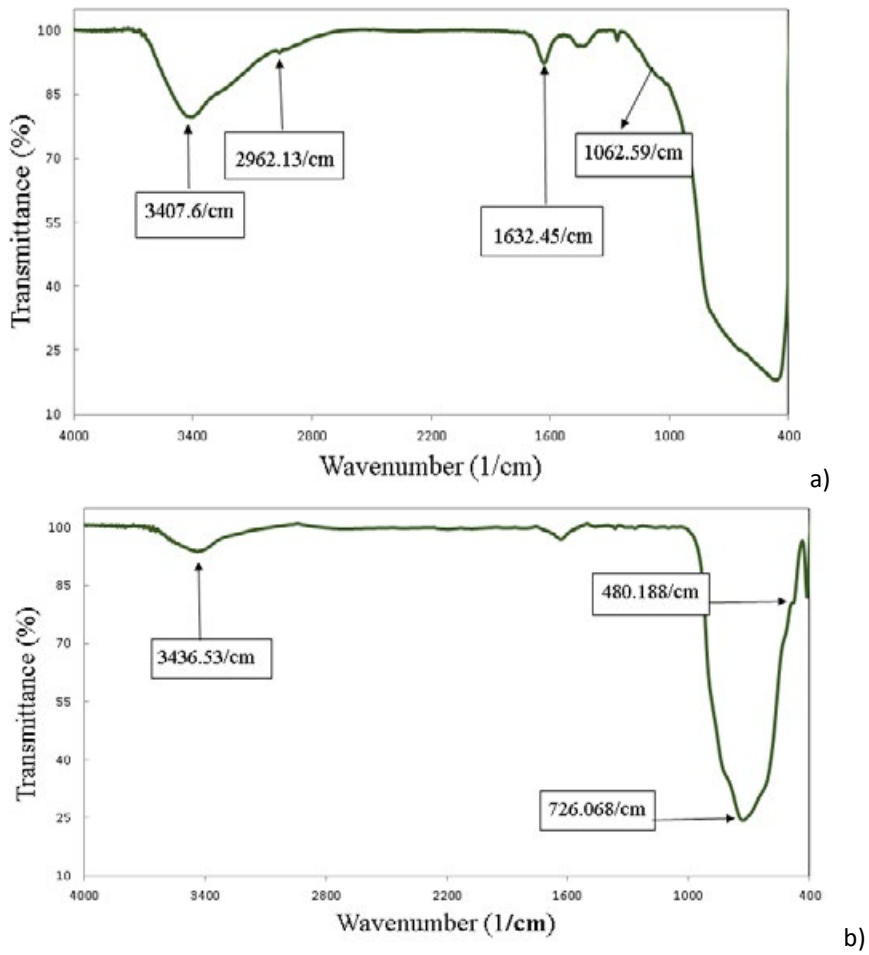

Fig. 5: FTIR (Fourier Transform Infrared Spectroscopy) spectra of: a) TiO_2, and b) $BiVO_4$

TiO_2, except that $BiVO_4$ is activated by visible light with no charge recombination (Fig. 8).

Comparison of AO10 removal at different initial concentrations

According to Fig. 9, the AO10 photodegradation decreases with the increase of its initial concentration. It seems that the main reason for the increase of initial concentration in dye is that its molecules are adsorbed more and more onto the surface of photocatalyst. High amount of dye concentration leads to reduction in generation of OH^* radicals on the surface of catalyst. In this condition, the terms of inhibitory effects on the reaction of dye molecules along with photogenerated holes or hydroxyl radicals may occur due to the fact that the active sites are covered by dye ions. Another reason that can be effective in removal efficiency at high concentrations of dye is the effect of UV screening. In this condition, a significant amount of UV may be absorbed by the dye molecules rather than the catalyst and the photons never reach the photocatalyst surface, leading to decrease of photocatalytic removal efficiency (Asiltürk *et al*., 2006; Konstantinou and Albanis, 2004; Nikazara *et al*., 2007; Pourata *et al*., 2009).

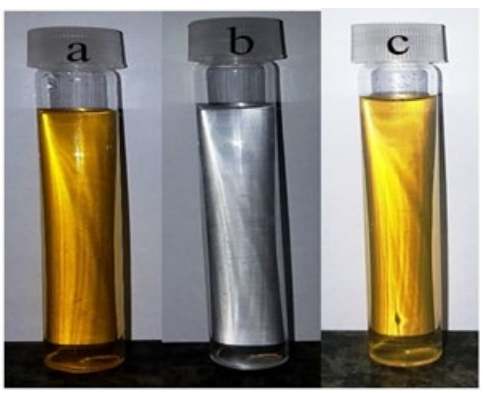

Fig. 6. The photographic representation of dye removal a) before, b) after using UV/TiO2, and c) after using UV–vis/BiVO4

Interactions of the studied variables in dye removal

Fig. 10a shows the percent of degradation efficiency for an irradiation time of 8 min and TiO_2 dosage of 0.25 g/100 mL obtained as a function of initial pH and initial dye concentration. The pH effect on the photocatalytic degradation of AO10 was investigated in the pH range of 1 to 13. An increase in AO10 dye degradation with the decrease of pH to below 7 can be explained by the UV/TiO_2 system in acidic solutions. A study by Shu and Chang (2005) showed the increase of efficiency by the decrease of pH to below 7. Hence, in acidic pH range, the dye will be predominantly in its protonated form, and its strong adsorption onto the TiO_2 surface and the corresponding high rate of degradation will occur. At these conditions, the surface will be positively charged and the TiO_2 surface can effectively adsorb the negatively charged dye anion (Gupta *et al*., 2012; Sakthivel *et al*., 2002; Gupta *et al*., 2016). At pH values of above 7, surface will negativity inhibit photocatalytic rates and lead

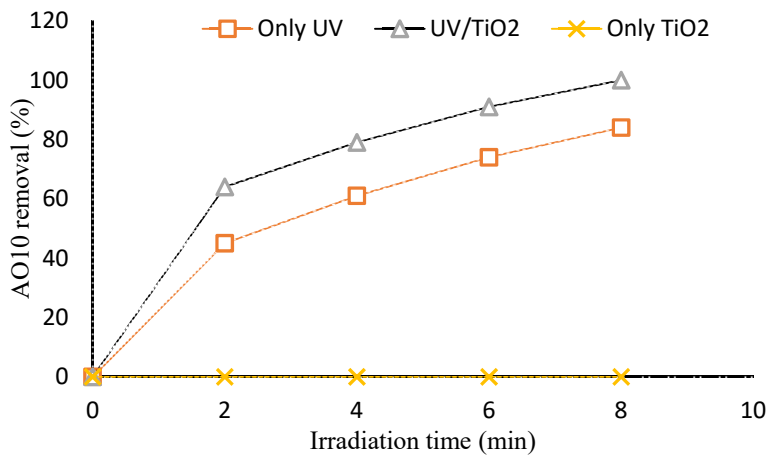

Fig. 7: Effect of TiO_2 on AO10 removal at different conditions as a function of irradiation time; [TiO_2] = 0.25 g/100 mL, dye concentration=10 mg/L, pH=3.5

Table 3: Experimental plan and results of the central composite design

Run order	A	B	C	D	Removal efficiency (%)			
					TiO_2		$BiVO_4$	
					Exp.	Pred.	Exp.	Pred.
1	0	0	0	2	77.88	75.02	9.97	9.97
2	2	0	0	0	99.76	97.36	9.97	9.97
3	-1	-1	-1	1	68.82	64.98	15.79	15.65
4	-1	1	1	-1	87.17	91.39	7.35	8.56
5	1	-1	1	-1	69.76	69.79	8.02	8.09
6	1	-1	-1	1	40.25	39.42	7.01	4.50
7	1	-1	-1	-1	33.55	30.86	6.21	5.13
8	-1	-1	-1	-1	58.23	57.82	10.94	10.51
9	0	0	0	0	69.22	69.22	9.97	9.97
10	-1	1	-1	-1	52.82	53.81	5.41	5.10
11	-1	-1	1	1	98.00	99.40	21.82	21.97
12	0	0	0	-2	63.94	61.75	4.44	4.50
13	0	0	0	0	69.22	69.22	9.97	9.97
14	0	0	0	0	69.22	69.22	9.97	9.97
15	1	1	1	-1	64.69	70.18	6.51	6.06
16	1	1	1	1	72.48	76.29	9.77	10.10
17	-1	-1	1	-1	94.00	93.78	14.29	14.73
18	1	-1	1	1	76.16	76.81	11.04	10.76
19	0	0	0	0	69.22	69.22	9.97	9.97
20	0	0	-2	0	0.000	2.30	0.000	2.02
21	-1	1	-1	1	56.70	60.06	11.76	11.59
22	0	-2	0	0	76.56	82.03	11.91	12.86
23	-1	1	1	1	91.76	96.10	5.41	5.10
24	0	2	0	0	88.00	77.49	7.03	6.78
25	0	0	2	0	84.61	77.27	11.87	10.55
26	0	0	0	0	69.22	69.22	9.97	9.97
27	0	0	0	0	69.22	69.22	9.97	9.97
28	2	0	0	0	53.23	50.59	7.11	8.77
29	1	1	-1	-1	27.64	29.63	4.10	3.85
30	1	1	-1	1	35.42	37.28	6.81	5.78

Table 4: Estimated regression coefficients for UV/TiO_2 process of AO10 removal

Factor	Coefficient	SE coefficient	*t*	*P*
Intercept	69.22	1.98	34.959	< 0.0001
A	-11.69	0.99	-11.808	< 0.0001
B	-1.13	0.99	-1.141	0.2691
C	18.74	0.99	18.929	< 0.0001
D	3.32	0.99	3.353	0.0043
AB	0.69	1.21	0.570	0.5746
AC	0.74	1.21	0.611	0.5490
AD	0.35	1.21	0.289	0.7760
BC	0.40	1.21	0.330	0.7436
BD	-0.23	1.21	-0.190	0.8530
CD	-0.39	1.21	-0.322	0.7544
A^2	1.19	0.92	1.293	0.2180
B^2	2.63	0.92	2.858	0.0121
C^2	-7.36	0.92	-8	< 0.0001
D^2	-0.21	0.92	-0.228	0.8251

to the decrease of the removal efficiency. Park *et al*. (2003) obtained the same result, in which the removal efficiency of dye decreased with the increase of pH to over 7. Some stuidies have shown that increase of pH to over 10 in solution favors OH^* formation on the catalyst surfaces and is directly responsible for initiating the dye oxidation (Lung-Chyuan and Tse-Chuan, 1993; Poulios and Aetopoulou, 1999). Dye

removal generally exhibits maximum decolorization at highly acidic or alkaline pH conditions. Fig. 10b displays the percent of degradation efficiencies for pH of 3.5 and TiO_2 dosage of 0.25 g/100 mL, obtained as a function of irradiation time and initial dye concentration. Equilibrium time can be considered as one of the most important design parameters in the photocatalytic process when a catalyst is used in the removal of organic pollutants. The plots illustrate that UV/TiO_2 has a high efficiency at all experimental intervals. The results revealed that 100% of AO10 dye was removed in 8 min. Fig. 10c illustrates the percent of removal efficiencies for an irradiation time of 8 min and pH of 3.5, obtained as a function of TiO_2 (g/100 mL) and initial dye concentration. The amount of catalyst loading is an important factor for detecting the adsorption capacity of solid for the removal of organic pollutants. Nanoparticle concentration has a great influence on the amount of decomposition in the presence of UV light, so that the removal efficiency increases in the range of 0.05 to 0.25 g/100 mL at a fixed amount of dye and contact time of 8 min. Abou-Gamra and Ahmed (2015) and Garcia and Takashima (2003) obtained similar results and concluded that the UV/TiO_2 process increased the removal efficiency of dye by increasing the catalyst dose.

Role of $BiVO_4$ in A010 degradation

Fig. 11 shows that with the increase of AO10 concentration, its decomposition decreases by irradiation time. However, the removal efficiency of this process was much lower than that of the UV/TiO_2

Table 5: Estimated regression coefficients for UV–Vis/$BiVO_4$ process of AO10 removal

Factor	Coefficient	SE coefficient	t	P
Intercept	25.27	7.74	3.264	< 0.0001
A	-1.07	0.19	-5.631	< 0.0001
B	-3.31	1.40	-2.364	0.0316
C	0.066	0.020	3.3	0.0048
D	92.59	38.49	3.353	0.0295
AB	0.069	0.018	2.405	0.0016
AC	-3.486	3.004	-1.160	0.2640
AD	-2.28	0.54	-4.222	0.0007
BC	-1.389	2.003	-0.693	0.4985
BD	4.53	3.60	1.258	0.2277
CD	0.12	0.060	0.2	0.0706
A^2	0.013	2.065	0.006	< 0.0001
B^2	-0.017	0.092	-0.184	0.8552
C^2	-1.138	2.549	-0.446	0.0005
D^2	-88.33	82.59	-1.069	0.3017

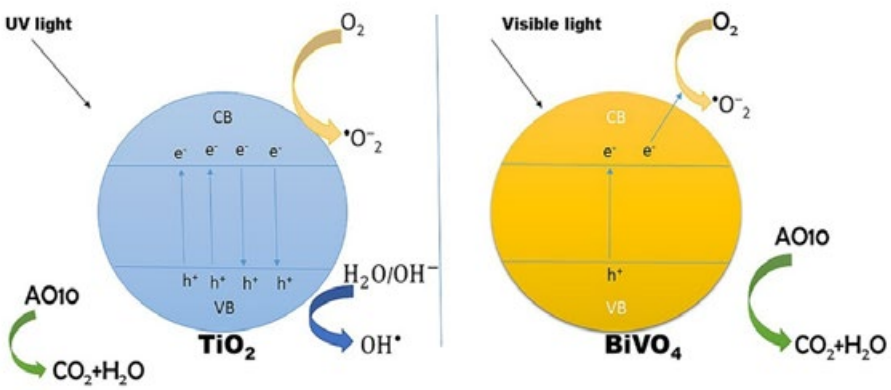

Fig. 8: Photocatalytic mechanism of TiO_2 and $BiVO_4$ nanoparticles
(Martinez-de La Cruz and Perez, 2010; Nakata and Fujishima, 2012; Roy *et al.*, 2011)

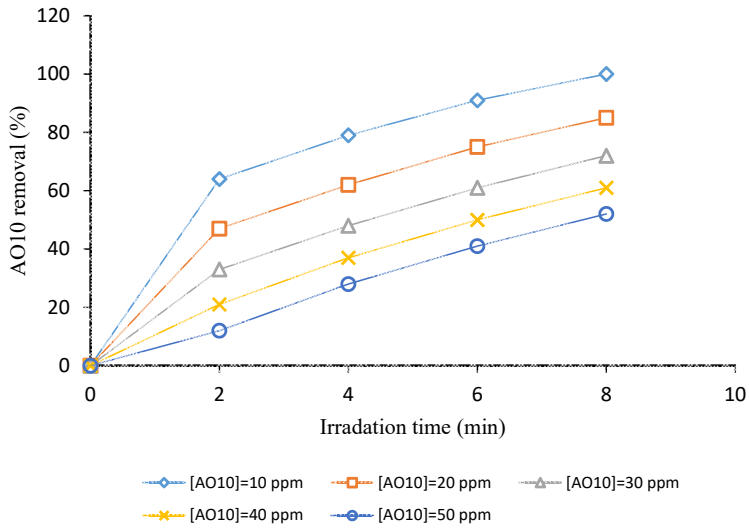

Fig. 9: Effect of initial concentration of AO10 on photo-oxidative removal of dye; [TiO_2] = 0.25 g/100 mL, pH=3.5

Table 6: Comparison of the two systems studied in this work with other processes

Catalyst	Light source	Dye concentration (mg/L)	Catalyst dosage (g/100 mL)	Time (min)	Efficiency (%)	References
ZnO	Solar	10	0.4	30	76.92	(Velmurugan and Swaminathan, 2011)
TiO_2	UV	30	0.1	120	99	(Toor *et al*., 2006)
TiO_2	UV	50	0.6	240	93	(Ong *et al*., 2012)
Ag_3VO_4	Visible	10	0.05	60	51	(Xu *et al*., 2010)
$BiVO_4$	Visible	10	0.08	360	46	(Li *et al*., 2016)
$BiVO_4$	Visible	10	0.06	180	30	(Shi *et al*., 2018)
PbWO4	UV	20	0.05	300	100	(Yu *et al*., 2013)
TiO_2	UV	11.88	0.17	12.87	100	The present study
$BiVO_4$	Visible	10.91	0.23	320.26	36.93	The present study

Table 7: Optimum values for degradation of AO10 dye by UV/TiO_2 and UV–Vis/$BiVO_4$ processes

Factors	Units	Optimum values	
		UV/TiO_2	UV–Vis/$BiVO_4$
Initial dye concentration	mg/L	11.88	10.91
Initial pH	-	4.59	3.23
Irradiation time	min	12.87	320.26
Catalyst dose	g/100 mL	0.17	0.23
Predicted degradation efficiency	(%)	100	36.93
Observed degradation efficiency	(%)	100	34.60

showed in Fig. 9. The photocatalytic capability of the synthesized catalyst $BiVO_4$ semiconductor was also investigated by the removal of AO10 under various conditions including pH values, dosage of catalyst, irradiation time and initial dye concentration. As shown in Fig. 12a, the pH range of 3 to 9 was investigated and higher dye removals were obtained at low initial pH values, especially pH 3. On the other hand, AO10 removal percent decreased with the increase of pH value and decolorization efficiency reached 26.7% at pH 9, irradiation time of 360 m, and catalyst dose of 0.25 g/100 mL. This can be attributed to the change

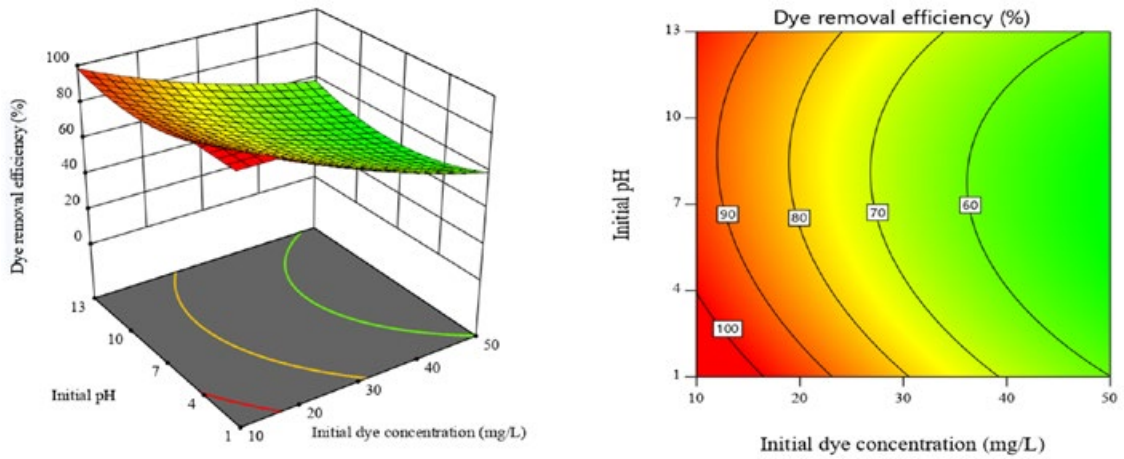

(a)

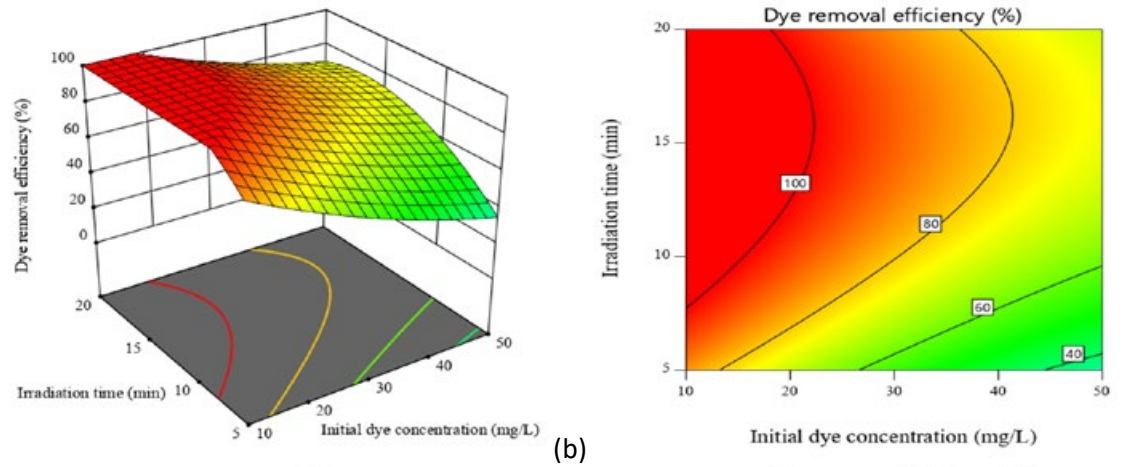

(b)

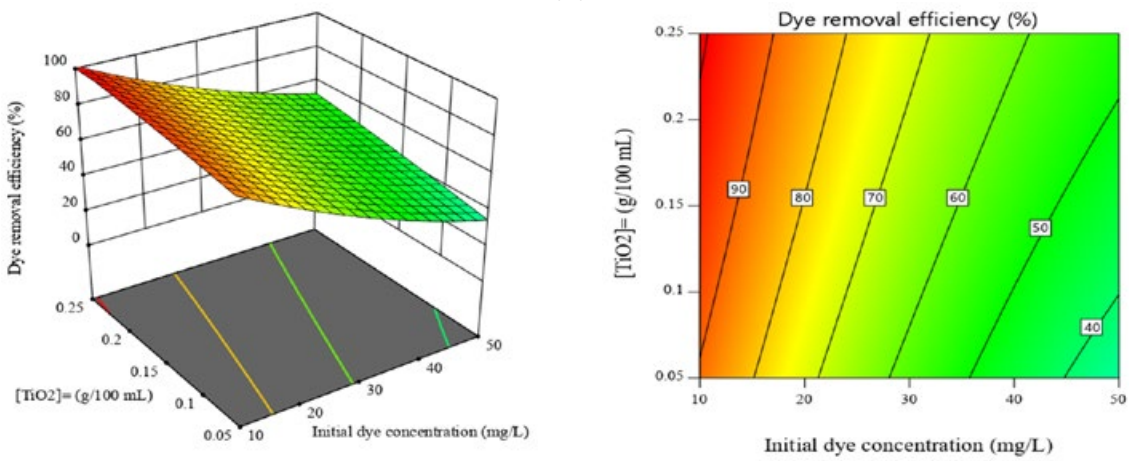

(c)

Fig. 10: The 3-D response surface and 2-D contour plot of dye removal efficiency (%) as a function of initial dye concentration (mg/L) in terms of a) initial pH b), irradiation time (min), and c) TiO_2 dosage (g/100 mL)

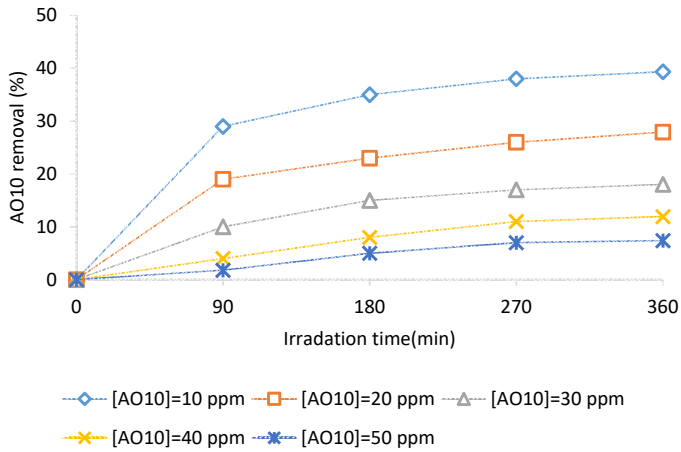

Fig. 11: Effect of initial concentration of AO10 on photo-oxidative removal of dye; [$BiVO_4$] = 0.25 g/100 mL, pH=3

in the surface charge of the adsorbent which can have a positive or negative charge at different pH values. However, experiments showed that the initial pH had no significant effect on AO10 dye removal. Fig. 12b shows the decrease of removal efficiency as only 39% of total AO10 was removed within 360 min. The increase of AO10 removal with the increase of time indicates the dye adsorption by the catalyst at higher contact times. The results presented in Fig. 12c indicate that decolorization efficiency increased with the increase of adsorbent dosage from 0.05 to 0.25 g/100 mL at pH 3. It is obvious that when the initial concentration of catalyst was increased, the reaction resulted in the highest removal efficiency. This could be attributed to the availability of larger surface area and more adsorption sites at higher adsorbent doses. Furthermore, the maximum dye removal efficiency occurred at the maximum catalyst dosage (0.25 g/100 mL), and decolorization efficiency decreased with the increase of the initial dye concentration. At the high dye concentration, the available active sites on the surface of catalyst are limited, leading to reduction of removal percentage in dye ions. Therefore, it can be concluded that the $BiVO_4$ semiconductor prepared by co-precipitation method has a little efficiency in AO10 degradation at all experimental intervals.

Comparison between the present study and previous studies

Table 6 compares the photocatalytic activity of the systems studied in this paper with other processes for the removal of dye reported in previous studies. As shown in Table 6, the rate of dye removal in the UV light with TiO_2 nanoparticle under optimum condition was remarkably higher than that of dye removal in other systems for degradation of dye. However, the rate of dye removal in UV–Vis/$BiVO_4$ process was low. Ong *et al*. (2012) observed 93% of 50 mg/L dye degradation during 240 min irradiation time in a UV light with 0.6 g/100 mL TiO_2. Around 76% of 10 mg/L dye was degraded in the photocatalytic process using ZnO catalyst under solar light within 30 min (Velmurugan and Swaminathan, 2011). The rate of 10mg/L dye degradation in a UV–Vis/Ag_3VO_4 process was observed to be 51% (Xu *et al*., 2010). This can be due to the fact that the TiO_2 nanoparticle is more efficient than other methods for enhancing photocatalytic activity for removing dye in the presence of UV light.

Determination of optimum conditions for TiO_2 and $BiVO_4$

Selection of the desired goal for each factor in terms of degradation efficiency was done based on "maximization" to obtain the maximum dye removal. Optimized values of the experimental design for TiO_2 and $BiVO_4$ are shown in Table 7. The actual values were in good agreement with the results achieved through RSM. In this way, the findings from optimization of the response surface were validated. According to the results obtained by the RSM model prediction and the experimental data validation, it can be concluded that the maximum degradation of AO10 is achieved using RSM.

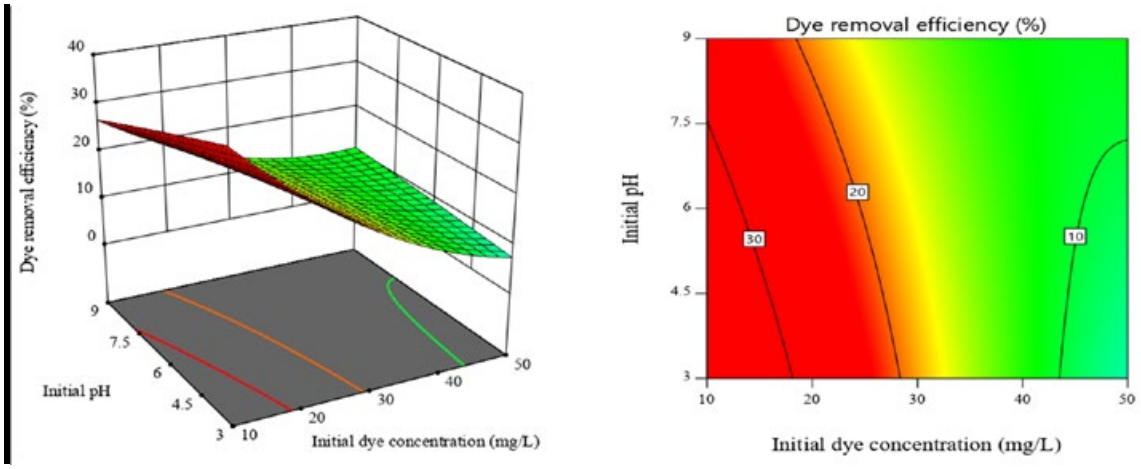

(a)

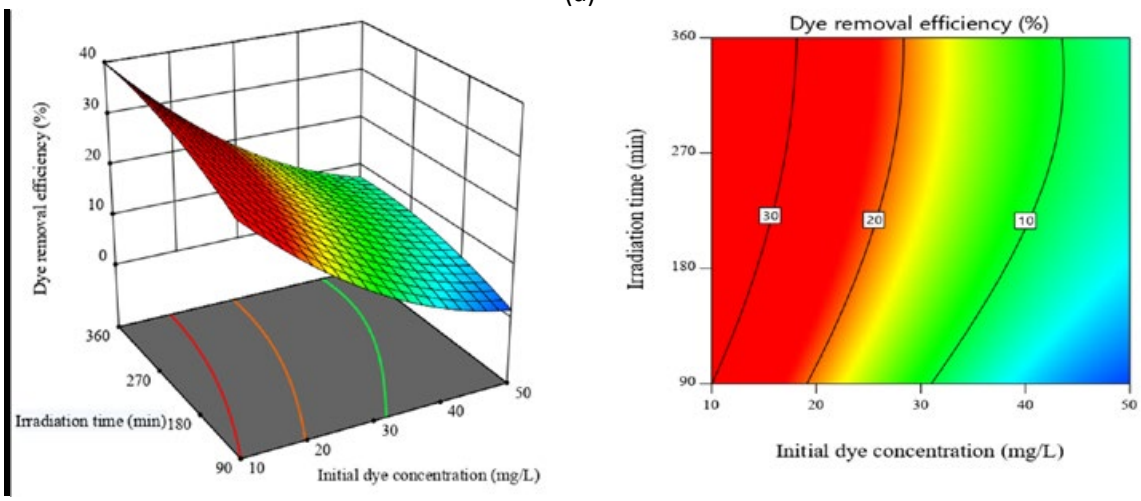

(b)

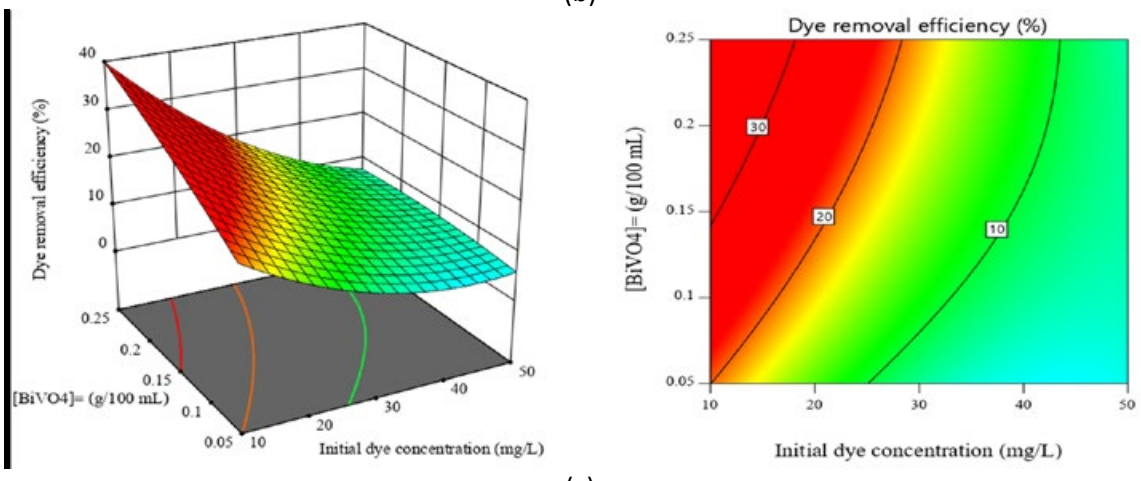

(c)

Fig. 12: The 3-D response surface and 2-D contour plot of the dye removal efficiency (%) as a function of initial dye concentration (mg/L) in terms of a) initial pH; b) irradiation time (min), and c) $BiVO_4$ dosage (g/100 mL)

CONCLUSION

The photocatalytic oxidation of AO10 was investigated by TiO_2 catalyst suspension and irradiation with a UV-C lamp (125 W) and $BiVO_4$ nanoparticles under visible light of an LED lamp (12 W). In the optimum conditions of process factors, the removal efficiencies of 100% and 36.93% were obtained for UV/TiO_2 and UV–Vis/$BiVO_4$ processes, respectively. According to the results, the degradation efficiency by TiO_2 as high as to remove all the dye in the solution, but the dye degradation efficiency using the synthesized $BiVO_4$ by co-precipitation method was low and incomplete. Therefore, it seems necessary to use the BiVO4 /TiO2 composite process to remove AO10 dye in further studies. The results obtained in this study showed that pH had not much effect on the AO10 removal process, and the dye can easily be removed at different pH values for both nanoparticles, especially TiO_2. Considering the limitations of traditional systems, application of RSM in optimization of design can effectively reduce the cost of expensive analytical methods and the related numerical disturbances. In the present study, it was indicated that RSM was an ideal method to optimize the independent variables and maximize the removal of dye.

ACKNOWLEDGEMENTS

This study is a postgraduate approved research project (No. 196213) performed at Isfahan University of Medical Sciences, Iran. The authors are sincerely thankful for the support of the Department of Environmental Health Engineering and Environment Research Center.

CONFLICT OF INTERESTS

The author declares that there is no conflict of interests regarding the publication of this manuscript. In addition, the ethical issues, including plagiarism, informed consent, misconduct, data fabrication and/or falsification, double publication and/or submission, and redundancy have been completely observed by the authors.

ABBREVIATIONS

2-D	2-dimentional
3-D	3-dimentional
A	Initial dye concentration (mg/L)
ABS_0^{475}	Absorbance at 475 nm before treatment
ABS^{475}	Absorbance at 475 nm after treatment
Ag_3VO_4	Silver vanadate(V)
AO10	Acid Orang10
B	pH
$BiVO_4$	Bismuth vanadate
C	Irradiation time (min)
CB	Conduction band
CCD	Central Composite Design
cm	Centimeter
Co.	Company
CO_2	Dioxide carbon
D	Catalyst dosage (g/100 mL)
DOE	Design of experimental
e_{CB}^-	Excited electron
Exp.	Experimental value
FE-SEM	Field-emission scanning electron microscope
Fig.	Figure
FTIR	Fourier Transform Infrared Spectroscopy
g	Gram
h^+	hole
HO	Hydroxide
H_2O	Water molecule
min	Minute
mL	Milliliter
mg/L	Milligram per liter
O_2	Oxygen molecule
$^{\bullet}O^-_2$	Oxygen radical
OH^*	Hydroxide radical
P	P value
$PbWO_4$	Lead tungstate
Pred.	Predicted value
RhB	Rhodamine B
ROS	Reactive Oxygen Species
RSM	Response surface methodology
SE	Standard error
t	T value
TiO_2	Titanium dioxide

UV	Ultra violet
VB	Valence band
Vis	Visible
x_0	The value of the x_i at the center point
x_i	Dimensionless coded value of an independent variable
XRD	X-ray diffraction
ZnO	Zinc oxide
Δx_i	Step change
β_0	Constant coefficient
β_i	Linear effect
β_{ii}	Quadratic effect
β_{ij}	Interaction effect
^oC	Celsius degrees
λ_{max}	Maximum wavelength
Y	Decolorization efficiency (%)
%	Percentage
µm	Micrometer

REFERENCES

Abou-Gamra, Z.M.; Ahmed, M.A., (2015). TiO_2 nanoparticles for removal of malachite green dye from waste water. Adv. Chem. Eng. Sci., 5(3): 373-388 (**16 pages**).

Aleboyeh, A.; Daneshvar, N.; Kasiri, M., (2008). Optimization of CI Acid Red 14 azo dye removal by electrocoagulation batch process with response surface methodology. Chem. Eng. Process.: Process Intensif., 47(5): 827-832 (**6 pages**).

Aravind, J., Kanmani, P., Sudha, G., Balan, R., (2016). Optimization of chromium(VI) biosorption using gooseberry seeds by response surface methodology. Global J. Environ. Sci. Manage., 2(1): 61-68 (**8 pages**).

Armağan, B.; Özdemir, O.; Turan, M.; Celik, M., (2003). The removal of reactive azo dyes by natural and modified zeolites. Chem. Technol. Biotechnol.,78(7): 725-732 (**8 pages**).

Asiltürk, M.; Sayılkan, F.; Erdemoğlu, S.; Akarsu, M.; Sayılkan, H.; Erdemoğlu, M.; Arpaç, E., (2006). Characterization of the hydrothermally synthesized nano-TiO_2 crystallite and the photocatalytic degradation of Rhodamine B. J. Hazard. Mater., 129(1): 164-170 (**7 pages**).

Bonyadinejad, G.; Sarafraz, M.; Khosravi, M.; Ebrahimi, A.; Taghavi-Shahri, S.; Nateghi, R.; Rastaghi, S., (2016). Electrochemical degradation of the Acid Orange 10 dye on a Ti/PbO_2 anode assessed by response surface methodology. Korean J. Chem. Eng., 33(1): 189-196 (**8 pages**).

Carmen, Z.; Daniel, A, S. Textile organic dyes–characteristics, polluting effects and separation/elimination procedures from industrial effluents–a critical overview. Organic pollutants ten years after the Stockholm convention-environmental and analytical update, 2012. InTech.

Chatchai, P.; Murakami, Y.; Kishioka, S.y.; Nosaka, A.Y.; Nosaka, Y., (2009). Efficient photocatalytic activity of water oxidation over $WO_3/BiVO_4$ composite under visible light irradiation. Electrochim. Acta., 54(3): 1147-1152 (**6 pages**).

Cho, I.H.; Zoh, K.D., (2007). Photocatalytic degradation of azo dye (Reactive Red 120) in TiO_2/UV system: Optimization and modeling using a response surface methodology (RSM) based on the central composite design. Dyes Pigm. , 75(3): 533-543 (**11 pages**).

Daneshvar, N.; Salari, D.; Khataee, A., (2003). Photocatalytic degradation of azo dye acid red 14 in water: investigation of the effect of operational parameters. J. Photochem. Photobiol., A. , 157(1): 111-116 (**6 pages**).

Daneshvar, N.; Hejazi, M.; Rangarangy, B.; Khataee, A., (2004). Photocatalytic degradation of an organophosphorus pesticide phosalone in aqueous suspensions of titanium dioxide J. Environ. Sci. Health., Part B., 39(2): 285-296 (**12 pages**).

Dawood, S.; Sen, T.K., (2012). Removal of anionic dye Congo red from aqueous solution by raw pine and acid-treated pine cone powder as adsorbent: equilibrium, thermodynamic, kinetics, mechanism and process design. Water Res. , 46**,** 1933-1946 (**14 pages**).

Dong, S.; Feng, J.; Li, Y.; Hu, L.; Liu, M.; Wang, Y.; Pi, Y.; Sun, J.; Sun, J., (2014). Shape-controlled synthesis of $BiVO_4$ hierarchical structures with unique natural-sunlight-driven photocatalytic activity. Appl. Catal., B., 152(413-424 (**12 pages**).

Fan, H.; Jiang, T.; Li, H.; Wang, D.; Wang, L.; Zhai, J.; He, D.; Wang, P.; Xie, T., (2012). Effect of $BiVO_4$ crystalline phases on the photoinduced carriers behavior and photocatalytic activity. J. Phys. Chem. C. , 116(3): 2425-2430 (**6 pages**).

Fujishima, A.; Rao, T.N.; Tryk, D.A., (2000). Titanium dioxide photocatalysis J. Phys. Chem. C ., 1(1): 1-21 (**21 pages**).

Garcia, J.C.; Takashima, K., (2003). Photocatalytic degradation of imazaquin in an aqueous suspension of titanium dioxide. J. Photochem. Photobiol., C ., 155(1): 215-222 (**8 pages**).

Gupta, V.K.; Jain, R.; Mittal, A.; Saleh, T.A.; Nayak, A.; Agarwal, S.; Sikarwar, S., (2012). Photo-catalytic degradation of toxic dye amaranth on TiO2/UV in aqueous suspensions. Mater. Sci. Eng., C . 32(1): 12-17 (**6 pages**).

Gupta, V.K.; Suhas; Tyagi,I.; Agarwal, S.; Singh, R.; Chaudhary, M.; Harit, A.; Kushwaha, S., (2016). Column operation studies for the removal of dyes and phenols using a low cost adsorbent. Global J. Environ. Sci. Manage., 2(1): 1-10 (**10 pages**).

Hoffmann, M.R.; Martin, S.T.; Choi, W.; Bahnemann, D.W., (1995). Environmental applications of semiconductor photocatalysis. Chem. Rev., 95(1): 69-96 (**28 pages**).

Hu, Y.; Li, D.; Wang, H.; Zeng, G.; Li, X.; Shao, Y., (2015). Role of active oxygen species in the liquid-phase photocatalytic degradation of RhB using BiVO4/TiO2 heterostructure under visible light irradiation J. Mol. Catal. A: Chem., 408(172-178 (**7 pages**).

Jiang, L. C.; Zhang, W.-D., (2010). Charge transfer properties and photoelectrocatalytic activity of TiO2/MWCNT hybrid. Electrochim. Acta, 56(1): 406-411 (**6 pages**).

Khataee, A.; Zarei, M.; Fathinia, M.; Jafari, M.K., (2011). Photocatalytic degradation of an anthraquinone dye on immobilized TiO2 nanoparticles in a rectangular reactor: Destruction pathway and response surface approach. Desalination, 268(1-3): 126-133 (**8 pages**).

Konstantinou, I.K.; Albanis, T.A., (2004). TiO2-assisted photocatalytic degradation of azo dyes in aqueous solution:

kinetic and mechanistic investigations: a review. Appl. Catal., B. 49(1): 1-14 (**14 pages**).

Li, W.; Wang, Z.; Kong, D.; Du, D.; Zhou, M.; Du, Y.; Yan, T.; You, J.; Kong, D., (2016). Visible-light-induced dendritic BiVO4/TiO2 composite photocatalysts for advanced oxidation process. J.All. Comp., 688: 703-711 (**9 pages**).

Liu, H.-L.; Chiou, Y.-R., (2005). Optimal decolorization efficiency of Reactive Red 239 by UV/TiO2 photocatalytic process coupled with response surface methodology. Chem. Eng. J. , 112(1-3): 173-179 (**7 pages**).

Lung-Chyuan, C.; Tse-Chuan, C., (1993). Photobleaching of methyl orange in titanium dioxide suspended in aqueous solution. J. Mol. Catal., 85(2): 201-214 (**14 pages**).

Martinez-de La Cruz, A.; Perez, U.G., (2010). Photocatalytic properties of BiVO4 prepared by the co-precipitation method: Degradation of rhodamine B and possible reaction mechanisms under visible irradiation Mater. Res. Bull. , 45, 135-141 (**7 pages**).

Montgomery, D.C., (2009). Design and analysis of experiments. John Wiley & Sons, New York. Design and analysis of experiments. 7th ed. John Wiley & Sons, New York.

Nakata, K.; Fujishima, A., (2012). TiO2 photocatalysis: Design and applications. J. Photochem. Photobiol., C , 13, 169-189 (**21 pages**).

Natarajan, K.; Bajaj, H.C.; Tayade, R.J., (2017). Direct sunlight driven photocatalytic activity of GeO2/monoclinic-BiVO4 nanoplate composites. Sol. Energy , 148: 87-97 (**11 pages**).

Ngah, W.W.; Teong, L.; Hanafiah, M., (2011). Adsorption of dyes and heavy metal ions by chitosan composites: A review. Carbohydr. Polym., 83, 1446-1456 (**11 pages**).

Nickheslat, A.; Amin, M.M.; Izanloo, H.; Fatehizadeh, A.; Mousavi, S.M., (2013). Phenol photocatalytic degradation by advanced oxidation process under ultraviolet radiation using titanium dioxide. J. Environ. Publ. Health, 2013.

Nikazara, M.; Gholivand, K.; Mahanpoor, K., (2007). Using TiO2 supported on clinoptilolite as a catalyst for photocatalytic degradation of azo dye disperse yellow 23 in water. Kinet. Catal. , , 48(2): 214-220 (**7 pages**).

Nong, L.; Xiao, C.; Jiang, W., (2011). Azo dye removal from aqueous solution by organic-inorganic hybrid dodecanoic acid modified layered Mg-Al hydrotalcite. Korean J. Chem. Eng., 28(3): 933-938 (**6 pages**).

Ong, S.-A.; Ho, L.-N.; Wong, Y.-S.; Min, O.-M.; Lai, L.-S.; Khiew, S.-K.; Murali, V., (2012). Photocatalytic mineralization of azo dye Acid Orange 7 under solar light irradiation. Des.Wat. Treat., 48(1-3): 245-251 (**7 pages**).

Park, J.-H.; Choi, E.; Gil, K.-I., (2003). Removal of reactive dye using UV/TiO2 in circular type reactor. J. Environ. Sci. Health., Part A. , 38(7): 1389-1399 (**11 pages**).

Pereira, L.; Pereira, R.; Oliveira, C.S.; Apostol, L.; Gavrilescu, M.; Pons, M.N.; Zahraa, O.; Madalena Alves, M., (2013). UV/TiO2 photocatalytic degradation of xanthene dyes. J. Photochem. Photobiol., 89(1): 33-39 (**7 pages**).

Poulios, I.; Aetopoulou, I., (1999). Photocatalytic degradation of the textile dye reactive orange 16 in the presence of TiO2 suspensions. Environ. Technol. , 20(5): 479-487 (**9 pages**).

Pourata, R.; Khataee, A.; Aber, S.; Daneshvar, N., (2009). Removal of the herbicide Bentazon from contaminated water in the presence of synthesized nanocrystalline TiO2 powders under irradiation of UV-C light. Desalination, 249(1): 301-307 (**7 pages**).

Rafatullah, M.; Sulaiman, O.; Hashim, R.; Ahmad, A., (2010). Adsorption of methylene blue on low-cost adsorbents: a review. J. Hazard. Mater., 177: 70-80 (**11 pages**).

Roy, P.; Berger, S.; Schmuki, P., (2011). TiO2 nanotubes: synthesis and applications. Angewandte Chem. Int. Ed. , 50: 2904-2939 (**36 pages**).

Saien, J.; Soleymani, A., (2007). Degradation and mineralization of Direct Blue 71 in a circulating upflow reactor by UV/TiO2 process and employing a new method in kinetic study. J. Hazard. Mater. 144(1): 506-512 (**7 pages**).

Sakthivel, S.; Shankar, M.; Palanichamy, M.; Arabindoo, B.; Murugesan, V., (2002). Photocatalytic decomposition of leather dye: comparative study of TiO2 supported on alumina and glass beads. J. Photochem. Photobiol. A., 148(1): 153-159 (**7 pages**).

Shi, L.; Xu, C.; Sun, X.; Zhang, H.; Liu, Z.; Qu, X.; Du, F., (2018). Facile fabrication of hierarchical BiVO 4/TiO 2 heterostructures for enhanced photocatalytic activities under visible-light irradiation. J. Mater. Sci., 53(16): 11329-11342 (**14 pages**).

Shu, H.-Y.; Chang, M.-C., (2005). Pilot scale annular plug flow photoreactor by UV/H2O2 for the decolorization of azo dye wastewater. J. Hazard. Mater., 125: 244-251 (**8 pages**).

Sohrabi, M.; Ghavami, M., (2008). Photocatalytic degradation of direct red 23 dye using UV/TiO2: effect of operational parameters. J. Hazard. Mater., 153: 1235-1239 (**5 pages**).

Sun, Y.; Qu, B.; Liu, Q.; Gao, S.; Yan, Z.; Yan, W.; Pan, B.; Wei, S.; Xie, Y., (2012). Highly efficient visible-light-driven photocatalytic activities in synthetic ordered monoclinic BiVO 4 quantum tubes–graphene nanocomposites. Nanoscale, 4: 3761-3767 (**7 pages**).

Tang, W.Z.; An, H., (1995). Photocatalytic degradation kinetics and mechanism of acid blue 40 by TiO2/UV in aqueous solution. Chemosphere, 31(9): 4171-4183 (**13 pages**).

Toor, A.P.; Verma, A.; Jotshi, C.; Bajpai, P.; Singh, V., (2006). Photocatalytic degradation of Direct Yellow 12 dye using UV/TiO2 in a shallow pond slurry reactor. Dyes. Pig., 68(1): 53-60 (**8 pages**).

Udom, I.; Ram, M.K.; Stefanakos, E.K.; Hepp, A.F.; Goswami, D.Y., (2013). One dimensional-ZnO nanostructures: synthesis, properties and environmental applications. Mater. Sci. Semicond. Process, 16(6): 2070-2083 (**14 pages**).

Vaez, M.; Zarringhalam Moghaddam, A.; Alijani, S., (2012). Optimization and modeling of photocatalytic degradation of azo dye using a response surface methodology (RSM) based on the central composite design with immobilized titania nanoparticles. Mater. Sci. Semicond. Process, 51(11): 4199-4207 (**9 pages**).

Velmurugan, R.; Swaminathan, M., (2011). An efficient nanostructured ZnO for dye sensitized degradation of Reactive Red 120 dye under solar light. Sol. Energy Mater. and Solar., 95(3): 942-950 (**9 pages**).

Venkatachalam, N.; Palanichamy, M.; Murugesan, V., (2007). Sol–gel preparation and characterization of alkaline earth metal doped nano TiO2: Efficient photocatalytic degradation of 4-chlorophenol. J. Mol. Catal. A: Chem., 273(1-2): 177-185 (**9 pages**).

Xu, H.; Li, H.; Sun, G.; Xia, J.; Wu, C.; Ye, Z.; Zhang, Q., (2010). Photocatalytic activity of La2O3-modified silver vanadates catalyst for Rhodamine B dye degradation under visible light irradiation. Chem. Eng.J., 160(1): 33-41 (**9 pages**).

Yingling, B.; Zongcheng, Y.; Honglin, W.; Li, C., (2011). Optimization

of bioethanol production during simultaneous saccharification and fermentation in very high-gravity cassava mash. Antonie van Leeuwenhoek, 99(2): 329-339 (**11 pages**).

Yu, C.; Cao, F.; Li, X.; Li, G.; Xie, Y.; Jimmy, C.Y.; Shu, Q.; Fan, Q.; Chen, J., (2013). Hydrothermal synthesis and characterization of novel PbWO4 microspheres with hierarchical nanostructures and enhanced photocatalytic performance in dye degradation. Chem. Eng. J., 219(86-95 (**10 pages**).

Zhang, A.; Zhang, J., (2009). The effect of hydrothermal temperature on the synthesis of monoclinic bismuth vanadate powders. Mater. Sci. Poland, 27: 1015-1023 (**9 pages**).

Zhang, L.; Long, J.; Pan, W.; Zhou, S.; Zhu, J.; Zhao, Y.; Wang, X.; Cao, G., (2012). Efficient removal of methylene blue over composite-phase BiVO4 fabricated by hydrothermal control synthesis. Mater. Chem. Phys., 136(2-3): 897-902 (**6 pages**).

Zhao, C.; Pelaez, M.; Dionysiou, D.D.; Pillai, S.C.; Byrne, J.A.; O'Shea, K.E., (2014). UV and visible light activated TiO2 photocatalysis of 6-hydroxymethyl uracil, a model compound for the potent cyanotoxin cylindrospermopsin. Catal. Today, 224: 70-76 (**8 pages**).

Zhu, J.; Yang, J.; Bian, Z.-F.; Ren, J.; Liu, Y.-M.; Cao, Y.; Li, H.-X.; He, H.-Y.; Fan, K.-N., (2007). Nanocrystalline anatase TiO2 photocatalysts prepared via a facile low temperature nonhydrolytic sol–gel reaction of TiCl4 and benzyl alcohol. Appl. Catal., B.I., 76(1-2): 82-91 (**10 pages**).

Zhu, Z.; Wu, R.-J., (2015). The degradation of formaldehyde using a Pt@TiO2 nanoparticles in presence of visible light irradiation at room temperature. J. Taiwan Inst. Chem. Eng., 50: 276-281 (**6 pages**).

AUTHOR (S) BIOSKETCHES

Rahimi, B., M.Sc. Student, Department of Environmental Health Engineering, School of Health, Isfahan University of Medical Sciences, Isfahan, Iran. Email: *b.r.rahimi17@gmail.com*

Ebrahimi, A., Ph.D., Associate Professor, Department of Environmental Health Engineering, School of Health, Isfahan University of Medical Sciences, Isfahan, Iran, and Environment Research Center, Research Institute for Primordial Prevention of Non-communicable disease, Isfahan University of Medical Sciences, Isfahan, Iran. Email: *a_ebrahimi@hlth.mui.ac.ir*

Mansouri, N., M.Sc. Student, Department of Environmental Health Engineering, School of Health, Isfahan University of Medical Sciences, Isfahan, Iran. Email: *y.mansouri72@gmail.com*

Hosseini, N., M.Sc. Student, Department of Environmental Health Engineering, School of Health, Isfahan University of Medical Sciences, Isfahan, Iran. Email: *niloofar.h.2969@gmail.com*

HOW TO CITE THIS ARTICLE

Rahimi, B.; Ebrahimi, A.; Mansouri, N.; Hosseini, N., (2019). Photodegradation process for the removal of acid orange 10 using titanium dioxide and bismuth vanadate from aqueous solution. Global J. Environ. Sci. Manage., 5(1): 43-60.

DOI: 10.22034/gjesm.2019.01.04

url: https://www.gjesm.net/article_33162.html